Chapter 1

Magnetic Field-Induced Strain of Metamagnetic Heusler Alloy $Ni_{41}Co_9Mn_{31.5}Ga_{18.5}$

Takuo Sakon, Naoki Fujimoto, Sho Saruki, Takeshi Kanomata, Hiroyuki Nojiri and Yoshiya Adachi

Additional information is available at the end of the chapter

http://dx.doi.org/10.5772/intechopen.76291

Abstract

$Ni_{41}Co_9Mn_{31.5}Ga_{18.5}$ is a re-entrant and metamagnetic Heusler alloy. In order to investigate the magnetic functionality of polycrystalline $Ni_{41}Co_9Mn_{31.5}Ga_{18.5}$, magnetic field-induced strain (MFIS) measurements were performed. A 0.12% MFIS was observed at 340 K and 10 T. Strict MFISs between 330 and 370 K were observed. These magneto-structural variances acted in concert with the metamagnetic property observed by the magnetization measurements and magneto-caloric property observed by the caloric measurements in applied magnetic fields. The MFISs were proportional to the fourth power of the magnetization, and this result is in agreement with Takahashi's spin fluctuation theory of itinerant electron magnetism. The investigation of time response of the MFIS was performed by means of water-cooled electric magnet, zero magnetic field to 1.66 T in 8.0 s at 354 K. A 2.2×10^{-4} MFIS was observed, which was 80% of the MFIS in a 60-s mode. This indicates that a high-speed transition has occurred on applying magnetic fields.

Keywords: magnetostriction, Heusler alloys, shape memory alloys, metamagnetic transition, itinerant magnetism

1. Introduction

In recent years, the ferromagnetic shape memory alloy (FSMA) was investigated as a candidate of the functional materials widely. Among FSMA, Ni_2MnGa is the most famous alloy [1]. The alloy has a cubic $L2_1$ Heusler structure (space group of $Fm\bar{3}m$), and ferromagnetic

transition realized [2, 3]. Cooling from room temperature, a martensite transition occurred at the martensitic transition temperature, T_M. Below T_M, a superstructure state occurred as a result of lattice deformation [4-6].

New alloys in the FMSAs of NiMnIn-, NiMnSn-, and NiMnSb-type Heusler alloys have been studied [7, 8]. In these alloys, a metamagnetic transition from paramagnetic martensite phase to ferromagnetic austenite phase occurred, and reverse martensitic transition, which was induced by magnetic fields, occurred under high magnetic fields [9, 10]. These alloys are hopeful as a metamagnetic shape memory alloys with a magnetic field-induced shape memory effect (MSIF) and as magnetocaloric materials which can be cooled down or heated up on applying external magnetic fields. It is noticeable that 3% MFIS has been observed for $Ni_{45}Co_5Mn_{36.7}In_{13.3}$ single crystal in compressive stress–strain measurements [11].

The Co-doped NiCoMnGa-type alloys turned the magnetic order of the parent phase from antiferromagnetic or paramagnetic phase, due to a large magnetization change across the transformation. As a result, it strengthens magnetic field driving force dramatically [12-24]. As for $Ni_{50-x}Co_xMn_{31.5}Ga_{18.5}$, the determined phases are a paramagnetic austenite (Para-A) phase, ferromagnetic austenite phase (Ferro-A), paramagnetic martensite phase (Para-M), and ferromagnetic martensite (Ferro-M) phase, with cooling from a higher temperature than T_C, which indicates re-entrant ferromagnetism [23].

Albertini et al. performed the experimental studies regarding the composition dependence of the structural and magnetic properties of the Ni-Mn-Ga ferromagnetic shape memory alloys substituting Co for Ni atoms around the composition of $Ni_{50}Mn_{30}Ga_{20}$ [12, 20]. The magnetic and structural properties indicated remarkable discontinuities around the martensitic transition. A metamagnetic transition appeared in the magnetic field around 400 K. The field dependence of the reverse martensitic transition temperature $dT_R/\mu_0 dH$ was −2.8 K/T and that of the thermal strain was reported. The most characteristic alloy is $Ni_{41}Co_9Mn_{32}Ga_{18}$. The magnetic susceptibility indicates a re-entrant magnetism property. We studied the magnetic properties of polycrystalline $Ni_{41}Co_9Mn_{31.5}Ga_{18.5.}$ Magnetization results indicated the metamagnetic transition between 330 and 370 K for 0–10 T. Moreover, a 0.1% magnetic field-induced strain (MFIS) was observed at the temperature of 340 K [23].

In our former article [25], we determined the magnetic field dependence of the magnetization of $Ni_{41}Co_9Mn_{31.5}Ga_{18.5}$ around the Curie temperature in the martensite phase in order to investigate the properties of the itinerant electron magnetism according to Takahashi's spin fluctuation theory of itinerant electron magnetism [26, 27]. The M^4 versus H/M plot was crossed across the coordinate axis at the Curie temperature in the martensite phase, T_{CM} = 263 K, and indicates a good linear relation behavior around T_{CM}. The results were in agreement with the Takahashi's theory concerning itinerant electron magnetism [26, 27]. Moreover, the spin fluctuation temperature T_A can be obtained from the M^4 versus H/M plot. The obtained T_A was 703 K. This value was much smaller than Ni (1.76×10^4 K). The value was comparable to that of UGe_2 (493 K), which is famous for the strongly correlated heavy fermion ferromagnet [27, 28].

Takahashi suggested that the anomalous behavior for the magnetostriction can be observed under the influence of the itinerant spin fluctuations around the critical temperature [27]. It is mentioned that the reason is that the magnetostriction is given by the volume derivative

of the free energy. By Eq. (6.101) of [27], the magnetostriction is proportional to the fourth power of the magnetization, M^4. The experimental magnetostriction study of weak itinerant ferromagnet MnSi was performed by Matsunaga et al. [29]. They plotted the magnetostriction against M^2. Around the Curie temperature, T_C = 30 K, the plot considerably deviated from the linearity. Takahashi mentioned that the linearity was confirmed by plotting the magnetostriction data against M^4 at T = 29 K around T_C.

In this chapter, we preformed MFIS measurements by means of a 10-T helium-free superconducting magnet and a 1.7-T water-cooled electric magnet. We compared the results of the strain and calorimetric differential scanning colorimetry (DSC) measurements and discussed the irreversibility of the MFIS and the reverse martensitic and metamagnetic transition. We investigated the correlations between magneto-structural variance and the magneto-caloric property observed by the caloric measurements in applied magnetic fields. It is interesting with the investigation of time response of the MFIS for the purpose of industrial use [30]. The time response of the MFIS performed by means of a 1.6-T water-cooled electric magnet and under atmospheric pressure, P = 0.1 MPa, was investigated. We also investigated the relation between the magnetostriction and the magnetization according to Takahashi's spin fluctuation theory of the itinerant ferromagnet for Ni_2MnGa and $Ni_{41}Co_9Mn_{31.5}Ga_{18.5.}$

2. Sample properties and experimental details

The crystal structure of $Ni_{41}Co_9Mn_{31.5}Ga_{18.5}$ is tetragonal DO_{22} structure, and the sample preparation of polycrystalline alloy was shown in our former article [23]. The nominal concentrations of the elements were Ni 41.0, Co 9.0, Mn 31.5, and Ga 18.5 at.%. The concentrations of the elements after thermal treatment are shown in **Table 1**. The ratio was almost the same as that of the nominal state. When cooling from 500 K, a ferromagnetic transition in the austenite phase was realized at T_C^A = 465 K. At the martensitic transition temperature, T_M = 315 K, the magnetization decreased drastically. The reverse martensitic transition temperature T_R was 380 K. The re-entrant magnetism, ferromagnetic-paramagnetic state, should be interacted with the crystal structures. The hysteresis of temperature, T_R - T_M was 65 K, which is much larger than that of other Ni_2MnGa-type alloys. This is due to the large motive force in order for a martensitic transition to occur [24].

MFIS measurements were performed with bulk samples with the size of 0.8 × 3.0 × 4.0 mm^3. Strain gauges were used (KFH-02-120-C1–16, size: sensor grid 0.2 mm length × 1.0 mm width, film base 2.5 mm length × 2.2 mm width, Kyowa Dengyo Co., Ltd., Yamagata, Japan). Strain gauge was fixed parallel to the long distance direction (4.0 mm) of the sample.

Ni	Co	Mn	Ga
40.8	9.0	31.5	18.7

Table 1. The concentrations of elements by means of EDS spectrometry (at. %).

External magnetic field was applied parallel to the long distance direction of the sample, and elongation of the sample was measured in applied magnetic fields and in atmospheric pressure. Measurements were performed by means of a 10-T helium-free magnet (10 T-CSM) at High Field Laboratory for Superconducting Materials, Institute for Materials Research, Tohoku University. We also performed MFIS measurements by means of a 1.7-T water-cooled electric magnet at Ryukoku University in order to investigate time response of MFIS. The magnetization measurements were performed by using a pulsed-field magnet with the time constant of 6.3 ms. The absolute value was calibrated against a sample of pure Ni.

3. Results and discussion

3.1. Relation between the magnetic field-induced strain and the magnetic entropy of $Ni_{41}Co_9Mn_{31.5}Ga_{18.5}$

In this section, we compared the results of the strain and calorimetric DSC measurements of $Ni_{41}Co_9Mn_{31.5}Ga_{18.5}$. We considered the correlation between the magnetic field-induced strain and the magnetic entropy.

Figure 1 shows the MFIS under steady field by means of the helium-free superconducting magnet. The MFIS measurements in this study were performed under atmospheric pressure and without the compression to make a pre-strain. The point zero of MFIS at each temperature is moved by 1×10^{-4} below 315 K and by 5×10^{-4} above 330 K. The thermal condition was the same as that for the magnetization measurement [23]. When increasing the magnetic field, distinct MFIS was observed. The maximum MFIS was 0.12%, which was approximately the same value as that of the thermal strain for the reverse martensitic transition. The shape of MFIS is similar to that of polycrystalline $Ni_{41}Co_9Mn_{32}Ga_{16}In_2$, where the alloy is also a re-entrant metamagnetic Heusler alloy, and 0.30% MFIS was observed [12]. The field dependence of the reverse martensitic transition temperature, $dT_R/\mu_0 dH$, are −7.9, −6.8, and − 4.8 K/T for $Ni_{41}Co_9Mn_{31.5}Ga_{18.5}$ [23], $Ni_{41}Co_9Mn_{32}Ga_{16}In_2$ [12], and $Ni_{45}Co_5Mn_{36.7}In_{13.3}$, respectively [11]. The field dependence of the reverse martensitic transition temperature of the ferromagnetic and non-metamagnetic Ni_2MnGa type alloys is between 0.2 and 1.0 K/T [2, 31, 32]. As for metamagnetic Heusler alloys, $dT_R/\mu_0 dH$ is much larger than that of non-metamagnetic Heusler alloys. Therefore, the MFIS occurs at a wide temperature range. The strain curves shown in **Figure 1** and the thermal strain in Ref. [23] suggest that the magneto-structural transition of $Ni_{41}Co_9Mn_{31.5}Ga_{18.5}$ alloy is very sensitive to magnetic fields. Below 330 K, the MFIS value returned to zero when a magnetic field became zero. By contrast, the MFIS value remained at the limit value without returning zero.

The MFIS of 2, 4, 6, and 8 T is shown in **Figure 2**. Between 340 and 370 K, large MFIS was observed. Metamagnetic S-shape like *M-H* curve was observed for the magnetization around 360 K [23]. The decreasing field process shows ferromagnetic behavior. Magnetization process indicates that the paramagnetic to ferromagnetic transition occurred. Considering the magnetization, MFIS indicates that the structural transformation from the paramagnetic martensite phase to the austenite ferromagnetic phase occurred. The MFIS and metamagnetism indicate

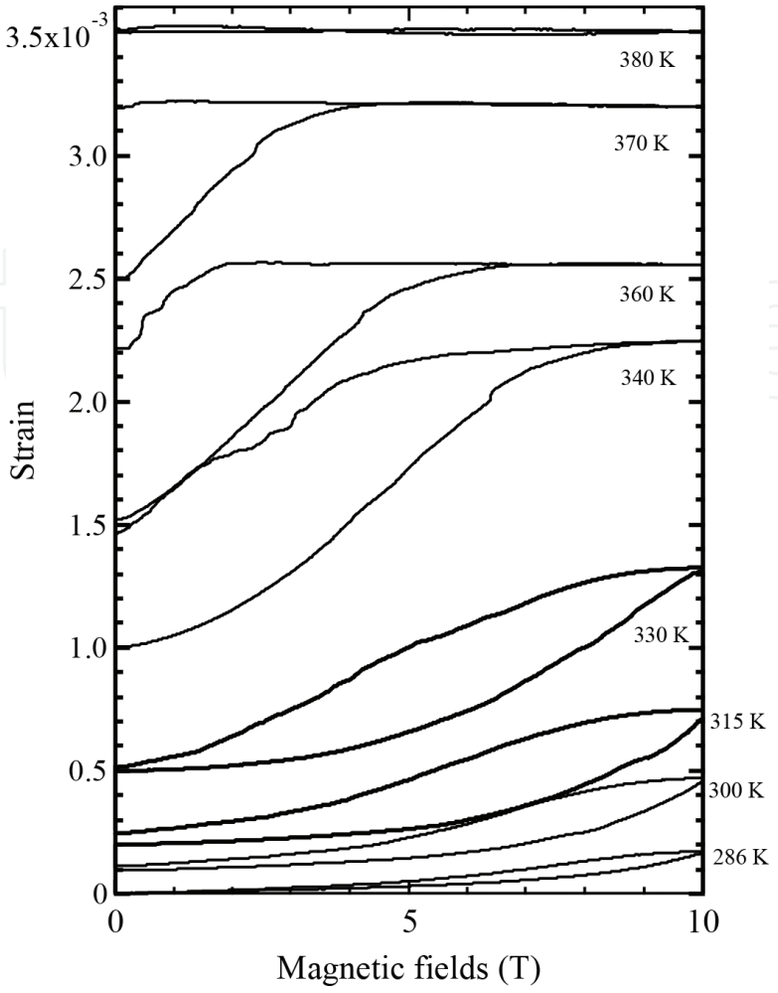

Figure 1. MFIS of $Ni_{41}Co_9Mn_{31.5}Ga_{18.5}$ in static magnetic fields. The point zero at each temperature is moved by 1×10^{-4} below 315 K and by 5×10^{-4} above 330 K.

that the magneto-structural coupling is large. The 0.12% (1200 ppm) MFIS is larger than the magnetostriction of TbDyFe single crystal under atmospheric pressure [33]. In this study, $Ni_{41}Co_9Mn_{38.5}Ga_{18.5}$ is a polycrystalline sample; then, it is easier to process and handle the sample than single crystals. **Table 2** indicates the thermal linear striction $\Delta L/L$(t), saturated magnetostriction $\Delta L/L$(m), and relative volume discontinuity at the martensitic transition, $\Delta V/V$.

In the former article, we studied the magneto-caloric properties of $Ni_{41}Co_9Mn_{31.5}Ga_{18.5}$ polycrystalline sample by means of the differential scanning calorimetry (DSC) measurements [25]. Magneto-calorimetric measurements and magnetization measurements of $Ni_{41}Co_9Mn_{31.5}Ga_{18.5}$ polycrystalline ferromagnetic shape memory alloy (FSMA) were performed across the T_R, at atmospheric pressure. When the sample was warmed from the martensite phase, a gradual increase in the thermal expansion due to the reverse martensitic transition at T_R was observed by the thermal expansion experimental study. These transition temperatures decreased steeply with an increasing magnetic field. The field dependence of the reverse martensitic transition temperature, $dT_R/\mu_0 dH$, is −7.9 K/T near zero fields. From the DSC measurements, the value of the latent heat was obtained as 2.6 kJ/kg in zero fields. The maximum value of

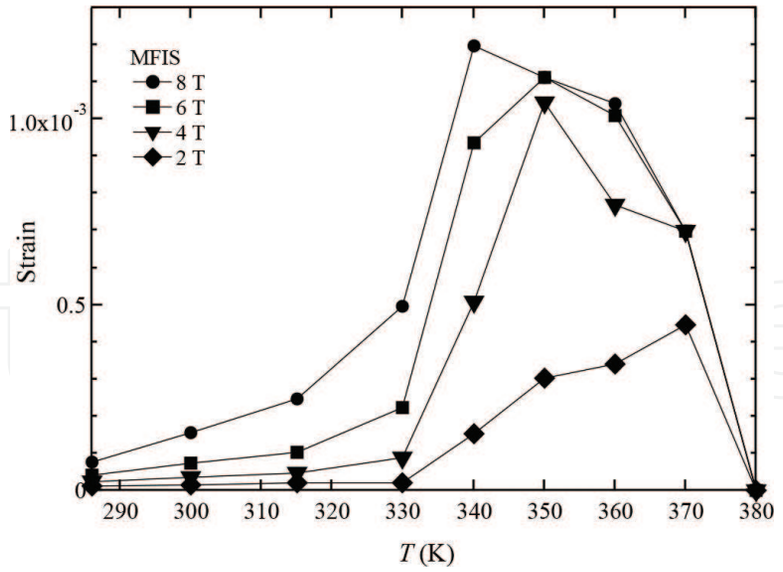

Figure 2. Field dependences of the MFIS of $Ni_{41}Co_9Mn_{31.5}Ga_{18.5}$. The values of MFIS at 350 K were quoted from our former result [23].

Alloys	$\Delta L/L$(t)	$\Delta L/L$(m)	$\Delta V/V$ (%)	Reference
$Ni_{41}Co_9Mn_{31.5}Ga_{18.5}$	1.1×10^{-3}	1.2×10^{-3}	~0.33	This work
$Ni_{41}Co_9Mn_{32}Ga_{16}In_2$	3.5×10^{-3}	3.0×10^{-3}	~0.9	[12]

Table 2. The thermal linear striction $\Delta L/L$(t), saturated magnetostriction $\Delta L/L$(m), and the relative volume discontinuity at the martensitic transition, $\Delta V/V$.

the entropy change ΔS was 7.0 J/kgK in zero fields, and with increasing magnetic fields, ΔS was gradually increased. The relative cooling power (RCP) is obtained by integration ΔS with the temperature. The RCP was 104 J/kg at 2.0 T, which was almost as same as the value with In-doped $Ni_{41}Co_9Mn_{32}Ga_{16}In_2$ alloy [12].

Now, we compare the results of the strain and calorimetric DSC measurements. **Figure 3** shows the temperature dependence of the MFIS and entropy change. The entropy change $\Delta S = S(6\text{ T}) - S(0\text{ T})$ was obtained from magnetization results and DSC results between zero field and 6 T, from the DSC results ΔS in steady fields [25].

ΔS shows a finite value above 330 K. On the contrary, the MFIS shows almost zero below 330 K. The reversible MFIS (magnetostriction) was observed below 330 K. Above 330 K, irreversible MFIS and S-shape like *M-H* curve were observed. Considering these results, in the irreversible region $T \geq 330$ K, metamagnetic and reverse martensitic transition occurred between the paramagnetic martensite and ferromagnetic parent austenite phases. Around T_R, large latent heat was observed by DSC measurement. The irreversible MFIS, S-shape like *M-H* curve, and the observation of latent heat indicates that this transition is first-order transition. Therefore, in the finite ΔS value region (330 K≤T≤ 390 K), irreversible and large MFIS can be observed. This result indicates the strong influence of magnetic fields for magneto-structural transformation.

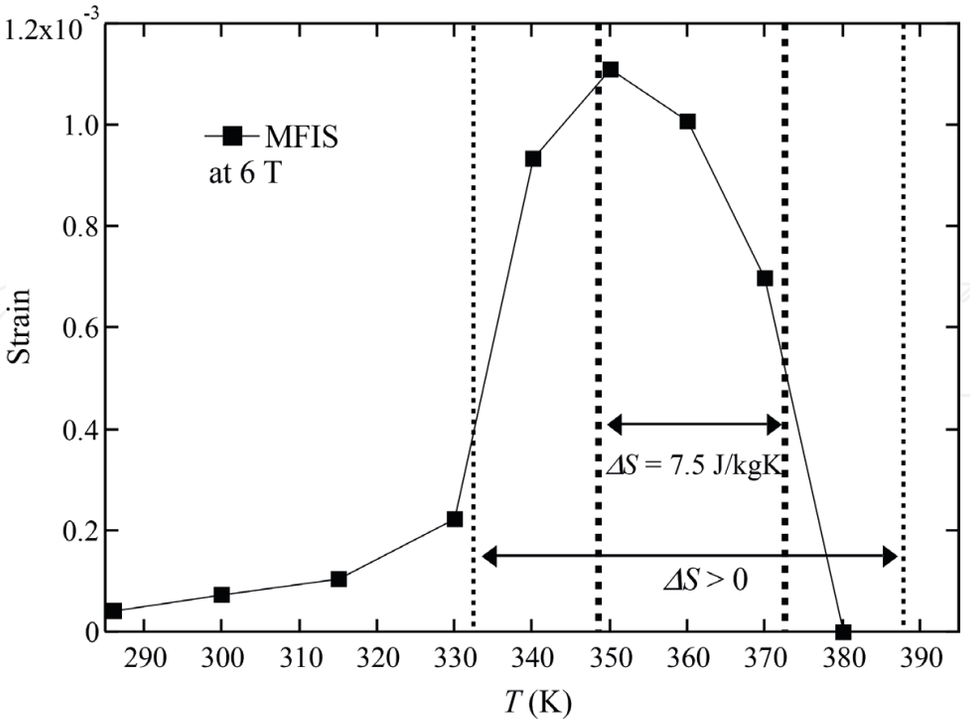

Figure 3. Temperature dependence of the MFIS at 6 T. Entropy change obtained from DSC results ΔS [29] between zero field and 6 T is also shown. Thin dotted lines indicate the area for $\Delta S > 0$. Bold dotted lines indicate the area for ΔS around 7.5 J/kgK.

3.2. Forced magnetostriction around the critical temperatures

In this section, we offer a topic of forced magnetostriction around the Curie temperature or magneto-structural transition temperature. The spin fluctuation theory of itinerant electron magnetism suggests that the critical index δ is defined by the critical magnetic isotherm function, $H \propto M^{\delta}$, where δ is around 5 [27]. Some scientists studied this relation concerning itinerant ferromagnetism. Nishihara et al. studied the magnetic field dependences of Ni and Ni_2MnGa [34]. As for Ni, the M^4 versus H/M plot shows the reasonable linear relation at the Curie temperature. The critical temperature of the spin fluctuation temperature, $T_{A,}$ was obtained as 1.76×10^4 K. This value is comparable with the value of 1.26×10^4 K, which was obtained by neutron diffraction experiments [35]. As for Ni_2MnGa, the critical index δ of the magnetic field dependence of the magnetization, $H \propto M^{\delta}$, at the Curie temperature was 4.70 ± 0.5 [34]. We measured the magnetization of Ni_2MnGa at the Curie temperature, $T_C = 375$ K. **Figure 4** presents the $M^{\delta-1}$ versus H/M plot. This figure indicates good linearity. These results indicate that the critical index δ of the magnetic field dependence of the magnetization is 4.70 and confirms the result of the former magnetization experiment.

In this study, we measured the magnetostriction of Ni_2MnGa at the Curie temperature in order to investigate the magnetization dependence of the forced magnetostriction. **Figure 5** presents the magnetostriction $\Delta L/L$ versus M^4 plot. The dotted line indicates a linear plot in order to guide the eyes. The result shows good linearity. It is considered that this result orders the Takahashi's spin fluctuation theory. The magnetization analysis of $Ni_{41}Co_9Mn_{31.5}Ga_{18.5}$ around the Curie temperature in the martensite phase according to the Takahashi's spin fluctuation theory was performed in the former article, as mentioned in Section 1 [25].

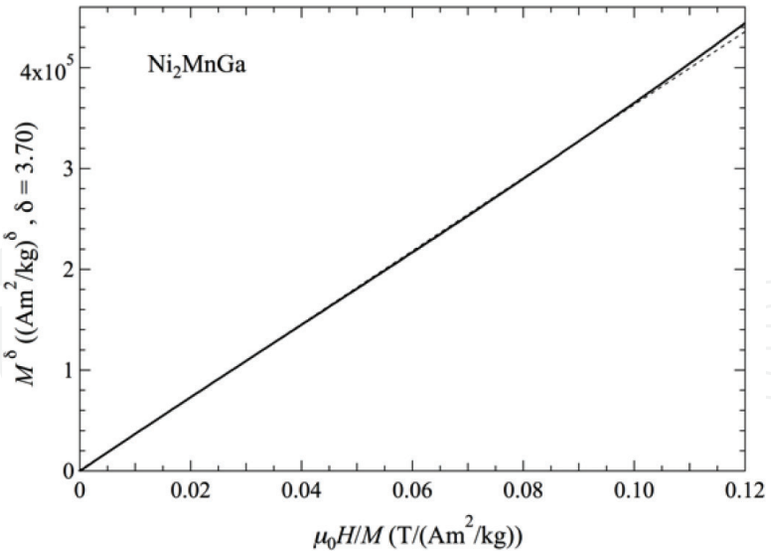

Figure 4. The $M^{3.7}$ versus H/M plot of Ni_2MnGa. The dotted line is a fitted linear line.

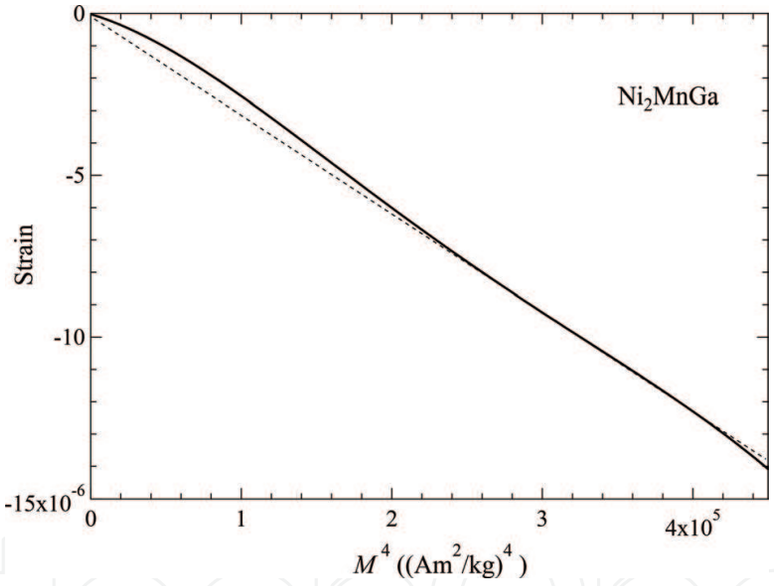

Figure 5. The magnetostriction $\Delta L/L$ versus M^4 plot of Ni_2MnGa. The dotted line is a fitted linear line.

We studied the magnetostriction at the Curie temperature in the martensite phase, $T_C^M = 263$ K. At this temperature, no structural phase transition occurred. Therefore, the striction under magnetic fields was decided as the magnetostriction. **Figure 6** shows the plot of the magnetostriction against M^2 at 263 K for $Ni_{41}Co_9Mn_{31.5}Ga_{18.5}$. The magnetostriction was not proportional to M^2. The plot was rounded. The plot of the numerically estimated magnetostriction at T_C was also rounded against M^2 [27]. **Figure 7** shows the plot of the magnetostriction against M^4 at 263 K. The dotted lines are linearly fitted lines. The fitted line passed the origin and shows good linearity, as that of Ni_2MnGa. It is conceivable that these results indicate that the magnetostriction is proportional to the fourth power of the magnetization, M^4.

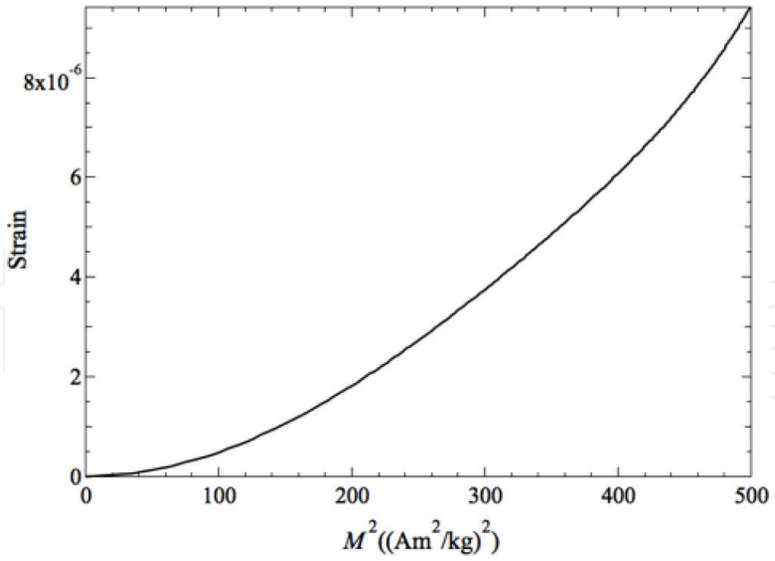

Figure 6. The plot of the magnetostriction against M^2 at 263 K for $Ni_{41}Co_9Mn_{31.5}Ga_{18.5}$.

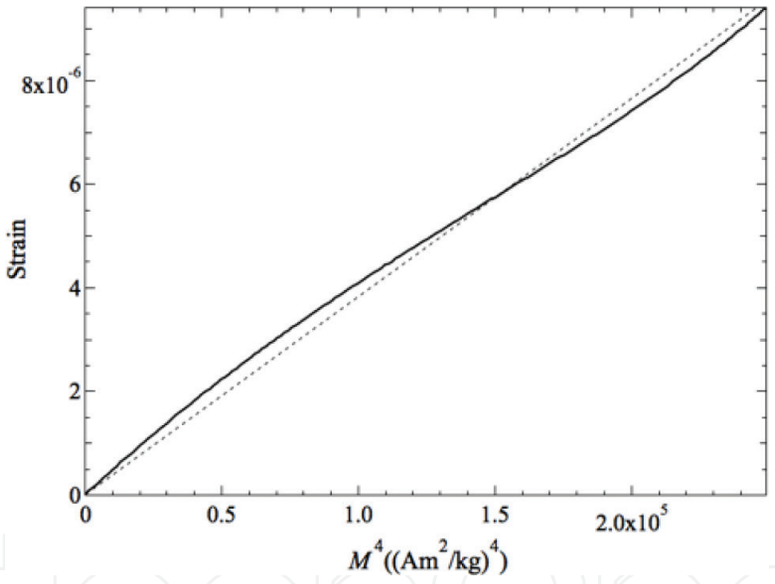

Figure 7. The plot of the magnetostriction against M^4 at 263 K for $Ni_{41}Co_9Mn_{31.5}Ga_{18.5}$. The dotted line is a fitted linear line.

Further, we investigated the MFIS around the reverse martensitic transition temperature. **Figures 8** and **9** show the magnetic field dependences of the magnetization and the MFIS at 330 and 340 K, respectively. These temperatures are around the reverse martensitic transition start temperature. The gradient of the magnetization and magnetostriction has tendencies toward increasing with the magnetic field increases for each temperature. However, the degree of the rate of increase of the magnetostriction is larger than that of the magnetization. From these figures, a correlation between the magnetostriction and magnetization could not be identified. As mentioned in Section 1, $Ni_{41}Co_9Mn_{31.5}Ga_{18.5}$ is an itinerant ferromagnet. The magnetostriction is proportional to M^4 at the Curie temperature in the martensite phase.

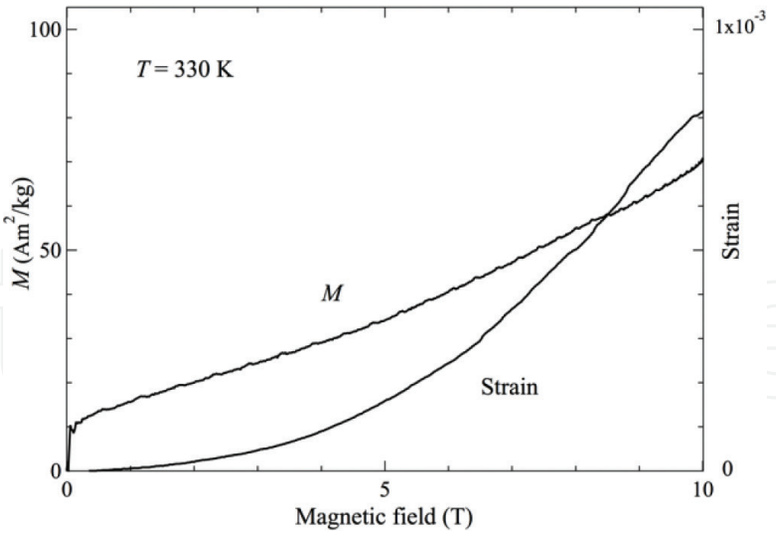

Figure 8. The magnetic field dependences of the magnetization and the MFIS at 330 K for $Ni_{41}Co_9Mn_{31.5}Ga_{18.5}$.

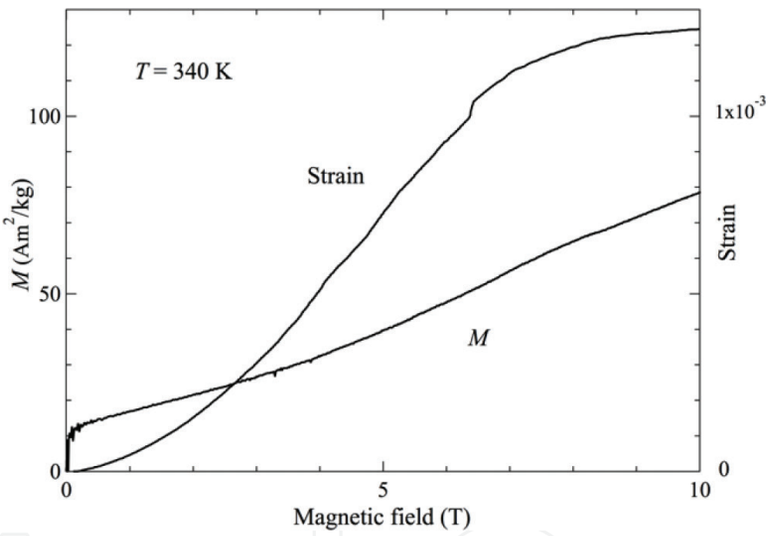

Figure 9. The magnetic field dependences of the magnetization and the MFIS at 340 K for $Ni_{41}Co_9Mn_{31.5}Ga_{18.5}$.

Therefore, it is presumed that the MFIS is also conformed to the power law suggested by Takahashi's theory.

Figure 10 shows the plot of MFIS against M^2 at 330 and 340 K. The dotted lines are linearly fitted lines. These fitted lines did not pass the origin, and the plot was rounded. **Figure 11** shows the plot of MFIS against M^4 at 330 and 340 K. The dotted lines are linearly fitted lines. These fitted lines passed the origin. It is conceivable that these results indicate that the MFIS is proportional to the fourth power of the magnetization, M^4, which was suggested by Takahashi's theory [27]. It is interesting that the M^4 behavior matures until 7 T at 330 K. At this temperature, magneto-structural transition (reverse martensitic and metamagnetic transition) occurred.

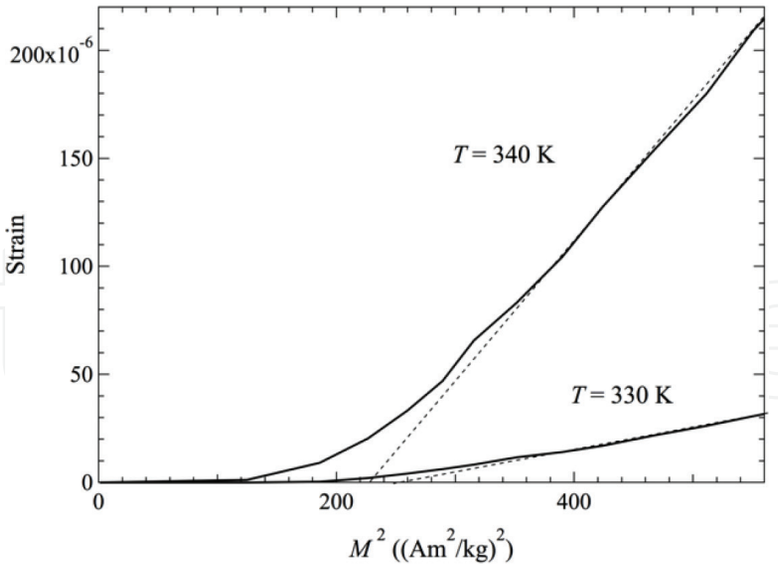

Figure 10. The plot of MFIS against M^2 at 330 and 340 K for $Ni_{41}Co_9Mn_{31.5}Ga_{18.5}$.

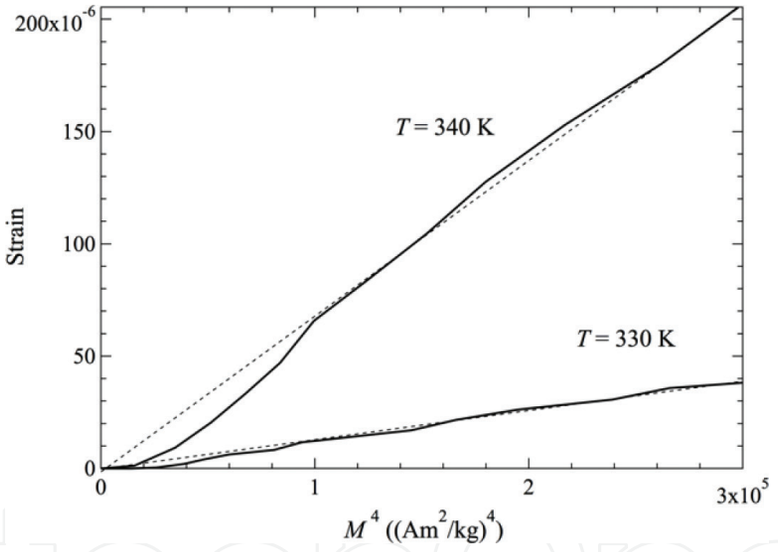

Figure 11. The plot of MFIS against M^4 at 330 and 340 K for $Ni_{41}Co_9Mn_{31.5}Ga_{18.5}$.

3.3. The time response of the magnetic field-induced strain of $Ni_{41}Co_9Mn_{31.5}Ga_{18.5}$

In order to investigate time response of the MFIS, fast speed sweeping of the magnetic fields was performed at 354 K, as shown in **Figure 12**. The applied magnetic field increased from the zero magnetic field to 1.66 T in 8.0 s and under atmospheric pressure. **Figure 13** shows the MFIS, in which the applied magnetic field increased from the zero magnetic field to 1.66 T in 60 s. As for an 8.0-s mode, 2.2×10^{-4} MFIS was observed, which was 80% of the MFIS in a 60-s mode. This indicates that a high-speed transition has occurred on applying magnetic fields.

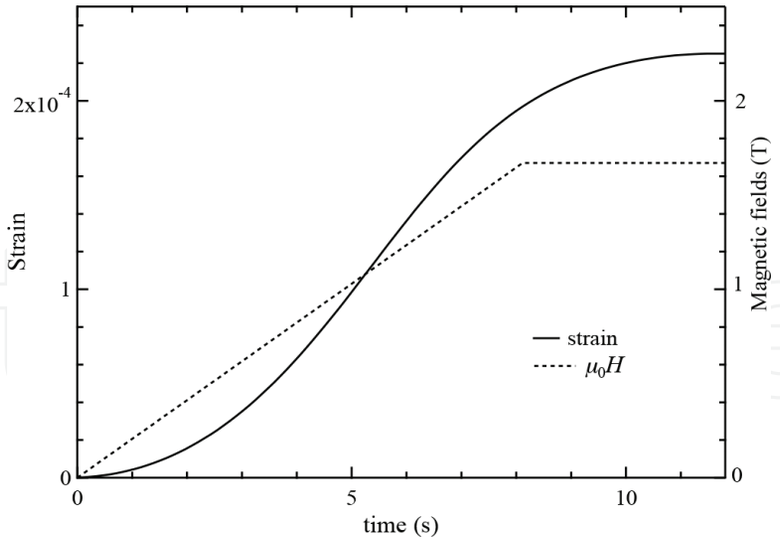

Figure 12. Time dependence of MFIS of $Ni_{41}Co_9Mn_{31.5}Ga_{18.5}$ at 354 K in increasing magnetic fields by means of a water-cooled magnet. The applied magnetic field increased from the zero magnetic field to 1.66 T in 8.0 s.

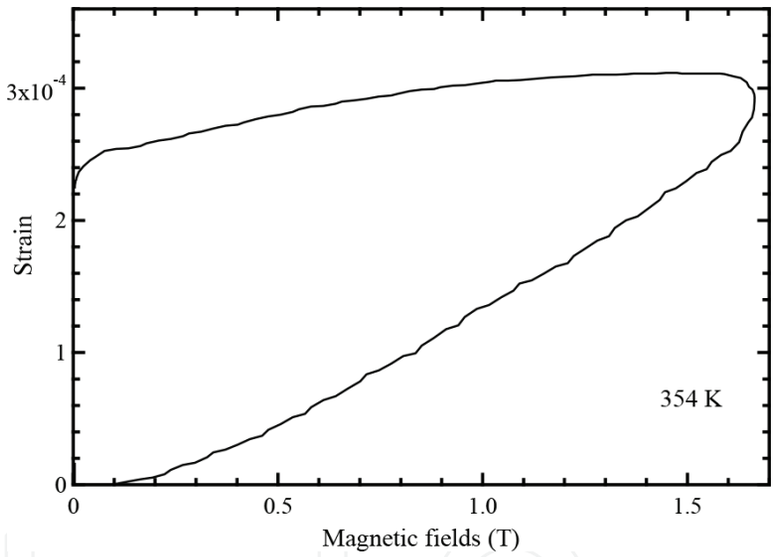

Figure 13. MFIS of $Ni_{41}Co_9Mn_{31.5}Ga_{18.5}$ at 354 K by means of a water-cooled magnet. The applied magnetic field increased from the zero magnetic field to 1.66 T in 60 s.

The MFIS effect occurs at the temperature between room temperature and 370 K; therefore, it is useful for magnetic sensors, or actuators in the high temperature region, *ex.* the engine room in the motor vehicles.

4. Conclusions

In order to investigate the magnetic functionality of polycrystalline metamagnetic Heusler alloy $Ni_{41}Co_9Mn_{31.5}Ga_{18.5}$, magnetic field-induced strain (MFIS) measurements were

performed. Strain gauge was fixed parallel to the long distance direction (4.0 mm) of the sample. The external magnetic field was applied parallel to the long distance direction of the sample, and the elongation of the sample was measured. A 0.12% MFIS was observed at 340 K and 10 T. Strict MFISs between 300 and 370 K were observed. These magneto-structural variances acted in concert with the metamagnetic property observed by the magnetization measurements and magneto-caloric property observed by the caloric measurements in the applied magnetic fields. The MFISs were proportional to the fourth power of the magnetization, and this result is in agreement with Takahashi's spin fluctuation theory of itinerant electron magnetism. The investigation of time response of the MFIS was performed by means of a sweep water-cooled electric magnet, and zero magnetic field to 1.66 T in 8.0 s at 354 K. 2.2×10^{-4} MFIS was observed, which was 80% of the MFIS in a 60-s mode. This indicates that a high-speed transition has occurred on applying magnetic fields.

Acknowledgements

The authors thank Mr. M. Okamoto for helping prepare equipment for MFIS measuring system. This experimental study was partly performed at High Field Laboratory for Superconducting Materials, Institute for Materials Research, Tohoku University.

Conflicts of interest

The authors declare no conflict of interest.

Author details

Takuo Sakon[1]*, Naoki Fujimoto[1], Sho Saruki[1], Takeshi Kanomata[2], Hiroyuki Nojiri[3] and Yoshiya Adachi[4]

*Address all correspondence to: sakon@rins.ryukoku.ac.jp

1 Department of Mechanical and System Engineering, Faculty of Science and Technology, Ryukoku University, Otsu, Shiga, Japan

2 Research Institute for Engineering and Technology, Tohoku Gakuin University, Tagajo, Miyagi, Japan

3 Institute for Materials Research, Tohoku University, Sendai, Miyagi, Japan

4 Graduate School of Science and Engineering, Yamagata University, Yonezawa, Yamagata, Japan

References

[1] Ullakko K, Huang JK, Kantner C, O'Handley RC, Kokorin VV. Large magnetic-field-induced strains in Ni_2MnGa single crystals. Applied Physics Letters. 1996;**69**:1966

[2] Webster PJ, Ziebeck KRA, Town SL, Peak MS. Magnetic order and phase transformation in Ni_2MnGa. Philosophical Magazine B. 1984;**49**:295

[3] Brown PJ, Crangle J, Kanomata T, Matsumoto M, Neumann K-U, Ouladdiaf B, Ziebeck KRA. The crystal structure and phase transitions of the magnetic shape memory compound Ni_2MnGa. Journal of Physics. Condensed Matter. 2002;**14**:10159

[4] Pons J, Santamarta R, Chernenko VA, Cesari E. Long-period martensitic structures of Ni-Mn-Ga alloys studied by high-resolution transmission electron microscopy. Journal of Applied Physics. 2005;**97**:083516

[5] Ranjan R, Banik S, Barman SR, Kumar U, Mukhopadhyay PK, Pandey D. Powder X-ray diffraction study of the thermoelastic martensitic transition in $Ni_2Mn_{1.05}Ga_{0.95}$. Physical Review B. 2006;**74**:224443

[6] Sakon T, Otsuka K, Matsubayashi J, Watanabe Y, Nishihara H, Sasaki K, Yamashita S, Umetsu RY, Nojiri H, Kanomata T. Magnetic properties of the ferromagnetic shape memory alloy $Ni_{50+x}Mn_{27-x}Ga_{23}$ in magnetic fields. Materials. 2014;**7**:3715

[7] Sutou Y, Imano Y, Koeda N, Omori T, Kainuma R, Ishida K, Oikawa K. Magnetic and martensitic transformations of NiMnX (X=In,Sn,Sb) ferromagnetic shape memory alloys. Applied Physics Letters. 2004;**85**:4358

[8] Oikawa K, Ito W, Imano Y, Sutou Y, Kainuma R, Ishida K, Okamoto S, Kitakami O, Kanomata T. Effect of magnetic field on martensitic transition of $Ni_{46}Mn_{41}In_{13}$ Heusler alloy. Applied Physics Letters. 2006;**88**:122507

[9] Umetsu RY, Kainuma R, Amako Y, Taniguchi Y, Kanomata T, Fukushima K, Fujita A, Oikawa K, Ishida K. Mössbauer study on martensite phase in $Ni_{50}Mn_{36.5}{}^{57}Fe_{0.5}Sn_{13}$ metamagnetic shape memory alloy. Applied Physics Letters. 2008;**93**:042509

[10] Khovaylo VV, Kanomata T, Tanaka T, Nakashima M, Amako Y, Kainuma R, Umetsu RY, Morito H, Miki H. Magnetic properties of $Ni_{50}Mn_{34.8}In_{15.2}$ probed by Mössbauer spectroscopy. Physical Review B. 2009;**80**:144409

[11] Kainuma R, Imano Y, Ito W, Morino YSH, Okamoto S, Kitakami O, Oikawa K, Fujita A, Kanomata T, Ishida K. Magnetic-field induced shape recovery by reverse phase transformation. Nature. 2006;**439**:957

[12] Albertini F, Fabbrici S, Paoluzi A, Kamarad J, Arnold Z, Righi L, Solzi M, Porcari G, Pernechele C, Serrate D, Algarabel P. Reverse magnetostructural transitions by Co and In doping NiMnGa alloys: Structural, magnetic, and magnetoelastic properties. Materials Science Forum. 2011;**684**:151

[13] Seguí C, Cesari E, Lázpita P. Magnetic properties of martensite in metamagnetic Ni–Co–Mn–Ga alloys. Journal of Physics D: Applied Physics. 2016;**49**:165007

[14] Kamarád J, Kaštil J, Skourski Y, Albertini F, Fabbrici S, Arnold Z. Magneto-structural transitions induced at 1.2 K in Ni_2MnGa-based Heusler alloys by high magnetic field up to 60 T. Materials Research Express. 2014;**1**:016109

[15] Seguí C. Effects of the interplay between atomic and magnetic order on the properties of metamagnetic Ni-Co-Mn-Ga shape memory alloys. Journal of Applied Physics. 2014;**115**:113903

[16] Entel P, Gruner ME, Comtesse D, Sokolovskiy VV, Buchelnikov VD. Interacting magnetic cluster-spin glasses and strain glasses in Ni–Mn based Heusler structured intermetallics. Physica Status Solidi B. 2014;**251**:2135

[17] Porcari G, Fabbrici S, Pernechele C, Albertini F, Buzzi M, Paoluzi A, Kamarad J, Arnold Z, Solzi M. Reverse magnetostructural transformation and adiabatic temperature change in Co- and In-substituted Ni-Mn-Ga alloys. Physical Review B. 2012;**85**:024414

[18] Segui C, Cesari E. Composition and atomic order effects on the structural and magnetic transformations in ferromagnetic Ni–Co–Mn–Ga shape memory alloys. Journal of Applied Physics. 2012;**111**:043914

[19] Kanomata T, Nunoki S, Endo K, Kataoka M, Nishihara H, Khovaylo VV, Umetsu RY, Shishido T, Nagasako M, Kainuma R, Ziebeck KRA. Phase diagram of the ferromagnetic shape memory alloys $Ni_2MnGa_{1-x}Co_x$. Physical Review B. 2012;**85**:134421

[20] Fabbrici S, Albertini F, Paoluzi A, Bolzoni F, Cabassi R, Solzi M, Righi L, Calestani G. Reverse magnetostructural transformation in Co-doped NiMnGa multifunctional alloys. Applied Physics Letters. 2009;**95**:022508

[21] Kihara T, Xu X, Ito W, Kainuma R, Adachi Y, Kanomata T, Tokunaga M. Magnetocaloric effects in metamagnetic shape memory alloys. In: Shape Memory Alloys—Fundamentals and Applications. Vol. 59-79. Croatia: InTech Publisher, Rijeka; 2017

[22] Yu SY, Cao ZX, Ma L, Liu GD, Chen JL, Wu GH, Zhang B, Zhang XX. Realization of magnetic field-induced reversiblemartensitic transformation in NiCoMnGa alloys. Applied Physics Letters. 2007;**91**:102507

[23] Sakon T, Sasaki K, Numakura D, Abe M, Nojiri H, Adachi Y, Kanomata T. Magnetic field-induced transition in Co-doped $Ni_{41}Co_9Mn_{31.5}Ga_{18.5}$ Heusler alloy. Materials Transactions. 2013;**54**:9

[24] Sakon T, Adachi Y, Kanomata T. Magneto-structural properties of Ni_2MnGa ferromagnetic shape memory alloy in magnetic fields. Metals. 2013;**3**:202

[25] Sakon T, Kitaoka T, Tanaka K, Nakagawa K, Nojiri H, Adachi Y, Kanomata T. Magnetocaloric and magnetic properties of meta-magnetic Heusler alloy $Ni_{41}Co_9Mn_{31.5}Ga_{18.5}$. In: Progress in Metallic Alloys. Rijeka, Croatia: InTech Publisher; 2016. p. 265

[26] Takahashi Y. Quantum spin fluctuation theory of the magnetic equation of state of weak itinerant-electron ferromagnets. Journal of Physics: Condensed Matter. 2001;**13**:6323

[27] Takahashi Y. Spin Fluctuation Theory of Itinerant Electron Magnetism. Berlin/Heidelberg, Germany: Springer-Verlag; 2013

[28] Sakon T, Saito S, Koyama K, Awaji S, Sato I, Nojima T, Watanabe K, Sato NK. Experimental investigation of giant magnetocrystalline anisotropy of UGe_2. Physica Scripta. 2007;**75**:546

[29] Matsunaga M, Ishikawa Y, Nakajima T. Magneto-volume effect of the weak itinerant ferromagnet MnSi. Journal of the Physical Society of Japan. 1982;**51**:1153

[30] Techapiesancharoenkij R, Kostamo J, Allen SM, O'Handley RC. Frequency response of acoustic-assisted Ni–Mn–Ga ferromagnetic-shape-memory-alloy actuator. Journal of Applied Physics. 2009;**105**:093923

[31] Gonzalez-Comas A, Obradó E, Mañosa L, Planes A, Chernenko VA, Hattink BJ, Labarta A. Premartensitic and martensitic phase transitions in ferromagnetic Ni_2MnGa. Physical Review B. 1999;**60**:7085

[32] Khovailo VV, Takagi T, Tani TJ, Levitin RZ, Cherechukin AA, Matsumoto M, Note R. Magnetic properties of $Ni_{2.18}Mn_{0.82}Ga$ Heusler alloys with a coupled magnetostructural transition. Physical Review B. 2002;**65**:092410

[33] Wang Z, Liu J, Jiang C, Xu H. The stress dependence of magnetostriction hysteresis in TbDyFe [110] oriented crystal. Journal of Applied Physics. 2011;**109**:123923

[34] Nishihara H, Komiyama K, Oguro I, Kanomata T, Chernenko V. Magnetization processes near the curie temperatures of the itinerant ferromagnets, Ni_2MnGa and pure nickel. Journal of Alloys and Compounds. 2007;**442**:191-193

[35] Takahashi Y. On the origin of the curie-Weiss law of the magnetic susceptibility in itinerant electron magnetism. Journal of the Physical Society of Japan. 1986;**55**:3533